



ChemComm

---

**Progress and Limitations in Reactive Oxygen Species  
Quantitation**

Journal:	<i>ChemComm</i>
Manuscript ID	CC-HIG-07-2024-003578.R1
Article Type:	Highlight

SCHOLARONE™  
Manuscripts

## Progress and Limitations in Reactive Oxygen Species Quantitation

Eleni M. Spanolios<sup>1</sup>, Riley E. Lewis<sup>1</sup>, Rhea N. Caldwell<sup>1</sup>, Safia Z. Jilani<sup>1</sup>, and Christy L. Haynes<sup>1\*</sup>

<sup>1</sup>University of Minnesota - Twin Cities

\*Corresponding author: chaynes@umn.edu

### Abstract

Reactive oxygen species (ROS) are a set of oxygen- and nitrogen-containing radicals. They are produced from a wide range of sources. In biological contexts, cellular stress leads to an overproduction of ROS which can lead to genetic damage and disease development. In industry, ROS are often productively used for water purification or for analyzing the possible toxicity of an industrial process. Because of their ubiquity, detection of ROS has been an analytical goal across a range of fields. To understand complicated systems and origins of ROS production, it is necessary to move from qualitative detection to quantitation. Analytical techniques that combine quantitation, high spatial and temporal resolution, and good specificity represent detection methods that can fill missing gaps in ROS research. Herein, we discuss the continued progress and limitations of fluorescence, electrochemical, and electron paramagnetic resonance detection of ROS over the last ten years, giving suggestions for the future of the field.

### Introduction

Reactive oxygen species (ROS) is an umbrella term used to describe a variety of nitrogen- and oxygen-based small molecules, often free radicals, including, but not limited to: hydroxyl radical ( $\cdot\text{OH}$ ), hydrogen peroxide ( $\text{H}_2\text{O}_2$ ), super oxide ( $\text{O}_2^{\cdot-}$ ), singlet oxygen ( $^1\text{O}_2$ ), nitric oxide ( $\text{NO}$ ), and peroxyxynitrite ( $\text{ONOO}^{\cdot-}$ ). They are characterized by their short lifetimes (most under several milliseconds) and high reactivity. ROS are commonly produced intracellularly through mitochondrial and respiratory pathways.<sup>1</sup> At low concentrations, ROS are critical to cellular communication; however, at high concentrations their rampant reactivity can cause several problems, such as genetic damage and cellular apoptosis.<sup>1-3</sup> Therefore, high concentrations of ROS are good indicators for various cellular diseases and can be correlated with cancerous tumors, neurological damage, aging, and a wide variety of other physiological and pathogenic disorders. Beyond human health relevance, ROS are widely studied within catalysis, water purification, agriculture, and for various industrial applications.<sup>4-8</sup> The ubiquity of ROS as a species of interest necessitates detection methods that operate in a range of conditions and with appropriate sensitivity and selectivity performance (**Figure 1**).

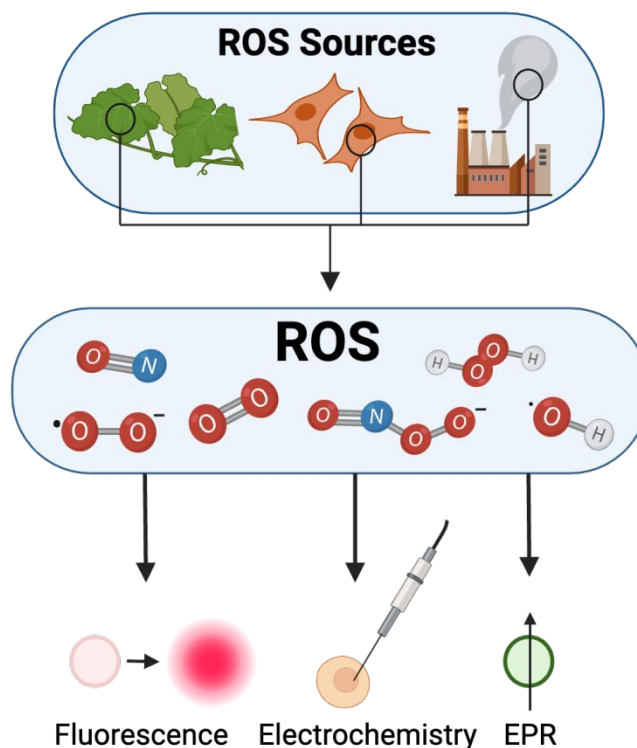


**Figure 1.** Overview of ROS generated by cells, for industrial processes like catalysis and water treatment, and in plant growth. Common ROS molecules are quantified by three main classes of techniques: fluorescence, electrochemistry, and electron paramagnetic resonance (EPR).

Detection of ROS has been historically difficult due to their short lifetimes, high reactivity, and the complex matrices in which they are produced and exist (Table 1). To overcome these challenges, a wide range of detection techniques are used to identify the presence of ROS. The most popular detection methods involve a variety of fluorescent probes such as Amplex Red and MitoSOX,<sup>9</sup> electrochemical techniques like amperometry and fast scan cyclic voltammetry (FSCV), and electron paramagnetic resonance spectroscopy (EPR).<sup>10</sup> Despite the vast array of techniques and instrumentation, none are universally effective for ROS detection, and quantifying ROS remains an analytical challenge.

Table 1. Common ROS lifetimes and oxidation potentials

Common ROS	H <sub>2</sub> O <sub>2</sub>	O <sub>2</sub> <sup>-</sup>	·OH	ONOO <sup>-</sup>	NO
Lifetime <sup>11</sup>	Several minutes	10 <sup>-6</sup> s	10 <sup>-9</sup> s	Several seconds	Several seconds
Oxidation Potential vs NHE at pH 7 <sup>12-14</sup>	0.38 V and 0.695 V	-0.16 V	2.32 V	1.4 V and 1.2 V	-0.8 V

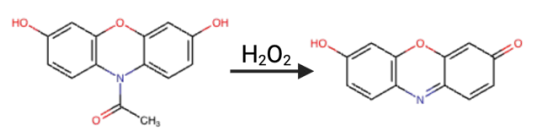
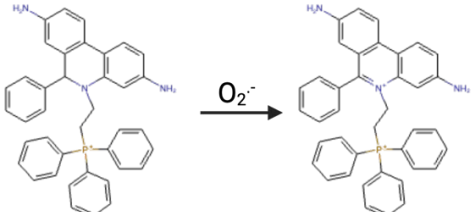
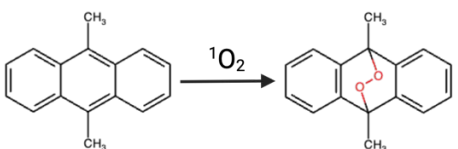
Quantitation is critical to piece together the entire picture of ROS production in a variety of applications. In cells, knowing the amount of ROS produced due to an exogenous stressor can provide valuable information on toxicity thresholds. In industry, understanding the quantity of ROS

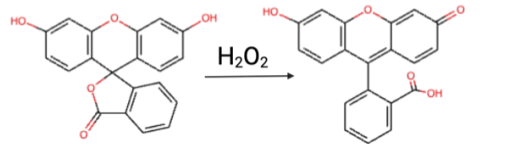
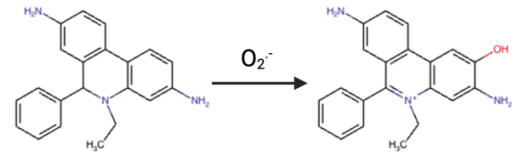
generated can provide insight on the efficiency of a water purification system. Coupling quantitation with specificity is especially useful to fully understand the production mechanism of a specific ROS and how to combat it or use it. An ideal ROS sensor should detect concentrations under 20  $\mu\text{M}$ , provide temporal resolution under one second, and display the highest level of spatial resolution possible.<sup>15</sup> Specific quantitation is often the missing piece of the ROS puzzle. In the past decade, several techniques have emerged to fill this detection gap and provide quantitative ROS sensors with a range of selectivity for specific species. This highlight discusses the most promising quantitative ROS sensors in a range of detection categories as well as limitations with which the field still struggles. We begin with limitations and advancements in quantitation using common fluorescent ROS probes. This is followed by electrochemical techniques and new electrode materials that have promoted lower limits of detection and greater selectivity for various ROS. EPR advances, specifically in probe design, are explored, and we end with further advances and suggested directions for the field.

### Fluorescence Direction:

Use of fluorescent probes are some of the most common methods for detecting ROS due to their simplicity, accessibility, and fast detection time. Traditional probes such as Amplex Red<sup>16, 17</sup>, dihydroethidium<sup>18, 19</sup>, dichlorofluorescein<sup>20</sup>, 9,9-dimethyl-9,10-dihydroacridine (DMA)<sup>21, 22</sup>, and their derivatives have been popular over the last decade. Most probes are oxidized by ROS through one-electron free radical reactions to produce stable fluorescent products. The specificity of these probes varies greatly, some react with select ROS while others detect overall levels of ROS. Table 2 describes the fluorescence mechanisms of common probes and the ROS they detect.

Table 2. Common ROS fluorescent probes

Probe Name	Fluorescence Mechanism	Species Detectable
Amplex Red		$\text{H}_2\text{O}_2$ , $\text{ONOO}^-$
MitoSOX		$\text{O}_2^-$
9,9-dimethyl-9,10-dihydroacridine (DMA)		$^1\text{O}_2$

Fluorescein		$\text{H}_2\text{O}_2$
Dihydroethidium (DHE)		$\text{O}_2^-$ , $\text{H}_2\text{O}_2$ , general ROS

Although fluorescent probes are widely used and accepted, they frequently suffer from poor biocompatibility, cell permeability, analyte specificity, stability, and quantitative capacity.<sup>23</sup> For example, Amplex Red is one of the most commonly used probes for  $\text{H}_2\text{O}_2$  detection in biological samples; however, it requires horseradish peroxidase and lacks cell permeability, making it unsuitable for studying endogenous intracellular processes.<sup>24</sup> Amplex Red is also not exclusively responsive towards  $\text{H}_2\text{O}_2$ ; it also reacts with peroxyxynitrite, requiring controls to exclude interferants in order to accurately estimate  $\text{H}_2\text{O}_2$ . Additionally, the stability of Amplex Red is pH- and concentration-dependent, rendering it unusable in overly acidic or basic environments.<sup>23, 25</sup>

For quantifying ROS with fluorescent probes, typically a calibration curve is created by exposing the probe to known ROS concentrations and monitoring the resulting fluorescence intensity. This calibration curve is later used to quantitate concentrations within more complex samples such as cells, tissue, or mixed media (**Figure 2**). However, the calibration curve solutions are often far less complex than the biological solutions relevant to ROS measurements. Therefore, they may not account for autooxidation or probe interferences that are common in more complex matrices. Certain probes, such as DCFH-DA, may also not correlate linearly with increased ROS, yielding further challenges in quantitation.<sup>26</sup> Additionally, translating solution-based calibration curves to imaging systems poses many difficulties, making fluorescence quantitation with spatial resolution nearly impossible. Therefore, these probes are good for observing changes to ROS in a system; however, they provide little avenue for gaining a deeper mechanistic understanding of ROS in a complex sample and struggle to provide absolute quantitation.

Recent research has indicated that many probes are much less specific than initially assumed and are highly susceptible to oxidation from non-ROS oxidants in biological systems.<sup>12</sup> For example, DCFH-DA is a commonly used cell-permeable probe; however, it does not react with superoxide,  $\text{H}_2\text{O}_2$ , or nitric oxide. Instead, the fluorescence signal results from oxidation by other potent oxidants and secondary reactions catalyzed by metal ions or heme proteins.<sup>26, 27</sup> The probe can also autooxidize from a variety of sources when in the one electron oxidized form, resulting in a self-amplified fluorescence signal. As a result, it is essential to employ careful controls for confident ROS quantitation, with some recommendations even stating that dyes alone are not enough to claim that ROS are present. Additionally, the probes have also been shown to be susceptible to transformation products of ROS.  $\text{H}_2\text{O}_2$  will break down into  $\cdot\text{OH}$ , so probes that reliably detect  $\cdot\text{OH}$  may also be detecting transformed  $\text{H}_2\text{O}_2$ , further limiting accurate quantitation and speciation.

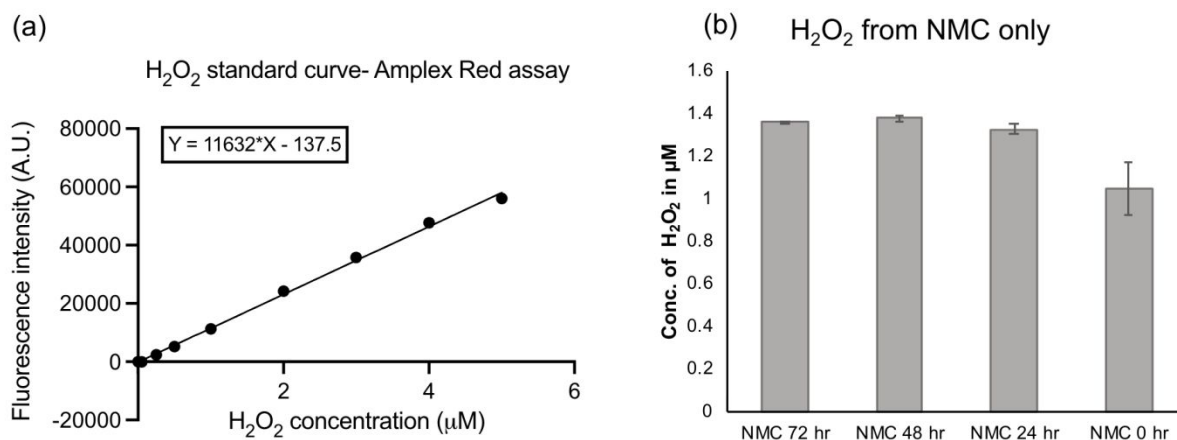


**Figure 2.** (a) To quantitate using a typical ROS fluorescence probe like Amplex Red, a calibration curve is made from standard additions of H<sub>2</sub>O<sub>2</sub>. (b) This calibration curve is used to quantify H<sub>2</sub>O<sub>2</sub> within a more complex solution, such as in a solution of nickel manganese cobalt oxide (NMC) nanoparticles.<sup>28</sup> Reprinted from ref 27 by permission of the publisher.

### Increasing Fluorescent Probe Specificity

While methodology and instrumentation for fluorescence-based ROS quantitation has not evolved radically, new fluorescent probes are regularly being developed. Probe development has greatly focused on increasing specificity as probes respond to various ROS and other biomolecules, making absolute quantitation nearly impossible. Without specificity, any signal will be comprised of both the analyte of interest and other interfering species. This fault becomes increasingly problematic when using fluorescent probes in mechanistic studies where multiple ROS coexist in the same environment. One way to overcome this limitation is through ratiometric probes.

Ratiometric probes emit two or more wavelengths where their intensities are analyte-dependent. These analyte signals are ratioed to correct for each other, which minimizes the effects of interference signals, can lower detection limits, and increase affinity towards specific ROS.<sup>29</sup> For example, Wu et al. developed a probe where, in the presence of superoxide, the fluorescence intensity at 483 nm increased with a simultaneous decrease in intensity at 378 nm.<sup>30</sup> This led to a superoxide-specific probe with a 7.4 μM limit of detection.

For probes with multiple emission wavelengths, combinations of different wavelength ratios may be tuned to detect various components and improve the probes' detection capabilities. Advances in the field include using ratiometric techniques to establish sensors with multiple analytical targets.<sup>31</sup> Cui et. al. developed a boron-substituted rhodamine probe that could detect and differentiate between H<sub>2</sub>O<sub>2</sub> and HOCl simultaneously.<sup>32</sup> In that work, they detect HOCl using a standard calibration curve and H<sub>2</sub>O<sub>2</sub> using ratioed signals. The resulting probe was highly specific with detection limits of 15 nM for H<sub>2</sub>O<sub>2</sub> and 10 nM for HOCl.<sup>33</sup>

Another way to overcome issues with specificity and interfering signals from additional ROS is by creating probes with more complex mechanisms. Liu et. al. recently developed a near-infrared Rhodal fluorophore probe (Rd-DPA3) that combined properties of both fluorescein and rhodamine dyes for *in vivo* imaging of ONOO<sup>-</sup> within a brain with confocal microscopy.<sup>34</sup> Here they implemented a "dual-lock-one-key" mechanism to improve the selectivity of the probe. The probe allows innovative measurement with its near-IR emission while being specific for ONOO<sup>-</sup> and passing through the blood brain barrier. To achieve this specificity, ONOO<sup>-</sup> first reacts with the aminophenol group on the probe to generate an alkylamine group, and then the ONOO<sup>-</sup> interacts

with the alkylamine group to turn on the probe. The resulting probe showed a 3.4 nM detection limit for  $\text{ONOO}^-$  with high specificity and minimal interference from other ROS and no noted decrease in temporal resolution (**Figure 3**). Excitation mechanisms with multiple steps like that of Rd-DPA3 are needed to get the level of selectivity required for confident ROS quantitation using fluorescence techniques.

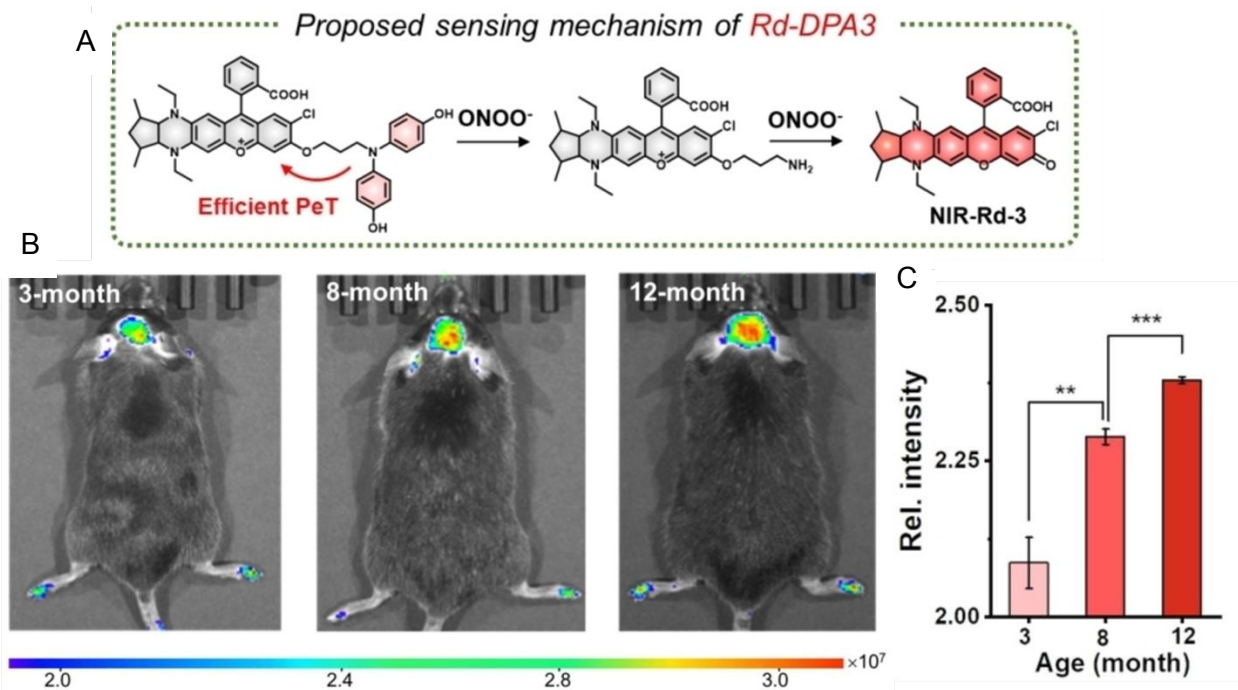


**Figure 3.** (A) The proposed, two-step sensing mechanism for  $\text{ONOO}^-$ . (B) Detection of  $\text{ONOO}^-$  in live mice at three different age groups using the Rd-DPA3 probe and the relative fluorescent intensities in each mouse age group. As the Alzheimer's-inflicted mice age, the quantity of  $\text{ONOO}^-$  in the brain increases.<sup>34</sup> Data cropped and reprinted from ref 32 by permission of the publisher.

Finally, Ding et. al worked to create probes sensitive to biogenic or abiogenic changes in tissue environments. They synthesized a pH-sensitive probe where the ROS affinity changes with a change in pH. They determined the limits of detection to be  $0.97 \mu\text{M}$  for  $\text{ONOO}^-$ ,  $0.17 \mu\text{M}$  for  $\text{ClO}^-$ , and  $0.20 \mu\text{M}$  for  $^1\text{O}_2$ .<sup>35</sup> This probe was used to detect inflamed tissues in mice using an imaging plate reader to monitor arthritis. This shows that it possible to detect different ROS in complex environments by manually altering the pH of a system to detect individual targets.

In addition to general fluorescence, ROS detection with super-resolution microscopy is being explored. Super-resolution microscopy allows for superior spatial enhancement as it overcomes the diffraction limit, thus allowing features much smaller than hundreds of nanometers to be resolved. Yang et. al used a cationic quinolinium-vinyl-N,N-dimethylaniline boronate derivative (QVD-B) probe that selectively fluoresces via three distinct modes for three distinct targets:  $\text{H}_2\text{O}_2$ , proteins, and nucleic acids.<sup>36</sup> The probe provided excellent selectivity and allowed for the high-resolution visualization of nucleoprotein dynamics in mitochondria. Although super-resolution microscopy provides the best optical spatial resolution available, it is currently challenging to quantify ROS from its fluorescence emission.

#### Fluorescent Chemosensors and Other Probe Advancements

Aside from enhancing probe specificity, other advancements have involved developing probes with larger Stoke shifts (the difference in wavelength between the absorption and emission spectra of a probe), improved kinetics, increased sensitivity, and higher photoluminescent quantum yields (PLQY).<sup>37, 38</sup> Using molecular design to increase the Stoke shift results in probes with more red-shifted emission, often in the near-infrared (NIR) and second near-infrared (NIR-II) window, leading to reduced interference with background autofluorescence, lessened light scattering, and lessened absorption by tissues.<sup>39</sup> Feng et al. developed a hydroxyl radical NIR-II probe with emission at 1044 nm and limit of detection of 0.5 nM that provides clear imaging of changing levels of hydroxyl radical within mouse organs.<sup>40</sup> Similarly, superoxide-specific NIR probes have been developed with emission at 716 nm and nM LODs.<sup>41</sup>

Likewise, there is great promise in the area of fluorescent chemosensors. These sensors contain a binding site that reacts with the analyte of interest, sometimes irreversibly. Due to the molecular interaction, the sensor can achieve higher specificity and enhanced fluorescent signals compared to other fluorescent probes.<sup>42-44</sup> There are a wide variety of fluorescent chemosensors that can detect ROS. While the specific molecular identity varies, typical ROS-detecting fluorescent chemosensors undergo chemical reactions with ROS to either release fluorescent molecules from the structure or undergo a molecular change that results in fluorescence. Examples can be found for a wide range of ROS, although many studies still suffer from the lack of quantitative capabilities common in other fluorescent probes. Common ROS detected in literature with fluorescent chemosensors include: ClO<sup>-</sup>, ONOO<sup>-</sup>, O<sub>2</sub><sup>-</sup>, H<sub>2</sub>O<sub>2</sub>, and NO.<sup>48, 49</sup> The most recent, quantitative, and high impact examples are described in detail below.

Hydrocyanine (hydro-Cy) is a reduced form of the commercially available cyanine dye. In 2009, it was discovered as a promising probe for ·OH and O<sub>2</sub><sup>-</sup>, two of the harder ROS species to detect.<sup>50</sup> Hydro-Cy reacts with ROS through a two-step electron transfer process to oxidize the dye back to the fluorescent cyanine form. There are several forms of these molecules including hydrocyanine-3, hydrocyanine-5, and hydrocyanine-7. These dyes vary in emission wavelength, where cyanine-7 fluoresces in the near-infrared and cyanine-3 fluoresces in the red region of the visible spectrum, two properties that are highly desirable for cellular probes. In addition to O<sub>2</sub><sup>-</sup> and ·OH, cyanine-3 (Cy3) and cyanine 5 (Cy5) have been used to quantify ONOO<sup>-</sup>. Jia et. al. describe a ratiometric probe that consists of both Cy3 and Cy5, operating on the principles of fluorescence resonance energy transfer (FRET).<sup>33</sup> This probe localizes in the mitochondria of cells, the main location of ONOO<sup>-</sup> production. Cy3 and Cy5 were linked together with acetyl-piperazyl-hexanoyl, with Cy3 acting as the FRET donor and Cy5 acting as the FRET acceptor, as seen in **figure 4**. Upon exposure to ONOO<sup>-</sup>, Cy3 does not very react due to a smaller polymethine chain, which allows for ratiometric analysis. A linear relationship between the ratio of Cy3 and Cy5 fluorescence was obtained for 0-700 nM ONOO<sup>-</sup> and was shown to be semi-quantitative in cells and highly selective for ONOO<sup>-</sup>.

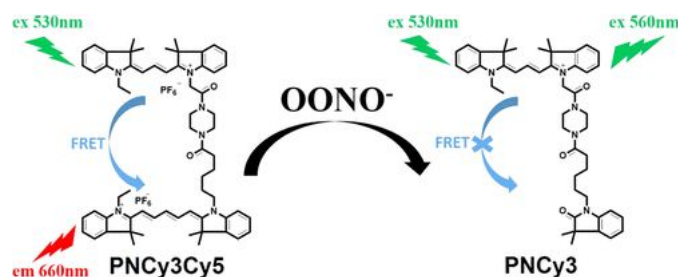


**Figure 4.** The basic FRET mechanism of the Cy3/Cy5 dyad for ONOO<sup>-</sup> detection.

Reprinted with permission from J. Am. Chem. Soc. 2016, 138, 10778–10781. Copyright 2016 American Chemical Society.



FRET is an increasingly common technique for ROS detection due to its ability to enhance signals and provide ratiometric analysis. Recently, Zhu et. al. described a rhodamine-based fluorophore for  $\text{ClO}^-$  detection.<sup>51</sup> In this example, a 1,8-naphthalimide donor was linked to a rhodamine B acceptor. To prevent cleavage of rhodamine, the diethylamino group in rhodamine B was replaced with a piperazine linker. Upon interaction with  $\text{ClO}^-$ , the rhodamine goes from a closed-ring to open-ring configuration, resulting in a fluorescent color change from blue to orange and a  $\text{ClO}^-$  detection limit of 4.50 nM. Rhodamine, in general, is a popular molecule for ROS detection, specifically because it lends itself towards ratiometric detection.<sup>52</sup>

Chemosensors are fruitful for ROS detection without FRET as well. Wang et. al. describe a chemosensor-based ratiometric probe for  $\text{H}_2\text{O}_2$  quantification.<sup>53</sup> One particularly large benefit of this work is the small probe concentrations required for ROS detection. This is critical for limiting disturbances that probe molecules can impose on biological systems, potentially causing additional ROS production and unreliable fluorescence results. To overcome this, they created a chemically induced dimerization-based amplifiable probe (CIDAP) that works at micromolar concentrations, allowing for the more accurate qualitative fluorescence readout. This probe was created by combining androgen receptors and a luciferase-based bioluminescence reporter, which is more sensitive than traditional fluorescent proteins. A smaller version of luciferase was developed to be used at picomolar concentrations for ROS detection. When cellular dihydrotestosterone is present, it triggers a homodimerization with the androgen receptors, triggering the bioluminescence. To quantify cellular  $\text{H}_2\text{O}_2$ , dose-response curves were created by measuring the signal collected from the addition of various quantities of dihydrotestosterone. This work successfully quantified  $\text{H}_2\text{O}_2$  in cells at a single micromolar level.

### *Nanoparticle Labels*

One emerging subfield in fluorescence quantitation makes use of fluorescent nanoparticles. Unlike most small-molecule probes, nanoparticles can have simple syntheses, readily tunable fluorescent properties, and high sensitivity. These probes don't rely on the molecular reactivity between a probe and ROS, but rather act as a label; as such, they aren't acting as ROS sensors but do contribute meaningfully to sensitivity. Unfortunately, some of these nanoparticles, like quantum dots, are likely to exhibit cytotoxic effects due to the heavy metal elements present in their structures.<sup>54, 55</sup> It is a common question if the addition of a probe to a biological system will set off further ROS production; therefore, known cytotoxicity makes these an impractical choice. Other nanoparticles may also induce ROS upon interaction with radiation, such as ultraviolet light or magnetic fields.<sup>56, 57</sup> Even with these limitations, some have achieved high specificity with fluorescent nanoparticles. Kailasa et. al. synthesized green fluorescent nanoclusters to specifically detect hydroxyl radicals in environmental water samples.<sup>58</sup> With a two-minute incubation time and a 9.13 nM detection limit, the probe works via a "turn-off" mechanism where the fluorescence is quenched in the presence of hydroxyl radicals. Although the probe is specific, "turn-off" mechanisms are far less desirable than probes that fluoresce upon interaction with ROS. "Turn-off" probes tend to be harder to reliably quantify and do not provide spatial detection information. In addition, it is common for multiple sources to cause fluorescence quenching while it usually takes a specific electron transfer reaction to cause a fluorophore to fluoresce or "turn on". Nanomaterials that facilitate ROS detection should continue to be pursued because of their high analytical performance capabilities and their accessibility.

## **Electrochemical Techniques**

Electrochemistry consists of several different techniques that rely on the electron transfer nature of the analyte. The redox-active nature of ROS makes them good candidates for

electrochemical detection. Electrochemical techniques such as amperometry and cyclic voltammetry (CV) are quantitative as the concentration of the analyte is proportional to the current detected. In addition to their quantitative nature, electrochemistry observes current changes in real-time and, depending on the size of the electrode and speed of detection, at high temporal resolution. This may allow for real-time detection of short-lived ROS.<sup>59-61</sup>

Most studies over the last ten years continue to use the classic techniques cyclic voltammetry, amperometry, or scanning electrochemical microscopy. CV is often diffusion-limited and tracks how current is changing over a range of potentials. This results in characteristic peaks representative of an analyte's oxidation or reduction potential within that specific electrolyte, at a specific temperature, and at a specific pH.<sup>62</sup> Therefore, each redox-active species theoretically has a distinct oxidation and reduction potential that can be captured independently from other species. To quantitate a species using CV, a calibration curve is typically generated ahead of unknown analyte measurement. Fick's law for mass transport diffusion describes a direct relationship between the activity of the analyte and the peak current in a voltammogram. The current intensity or the current density (current intensity divided by electrode area) is graphically compared to the concentration of the analyte of interest in the solution and, from the slope of the linear range, the limit of detection for the analyte in a specific electrochemical system is determined (**Figure 5**). To enhance temporal and spatial resolution, several labs use fast scan cyclic voltammetry (FSCV) for ROS detection.<sup>63</sup> The working electrode size is decreased to several microns or less in diameter to enhance spatial resolution, and the scan rate is increased to 100s of volts per second from a more common 10 millivolts per second, enhancing temporal resolution.<sup>64</sup> Using FSCV, detection limits can drop to nanomolar levels, shorter lived species can be detected in real time at microsecond temporal resolution, and single cell and tissue studies are possible due to the small size of the electrode. Quantitation works the same way as in traditional CV.

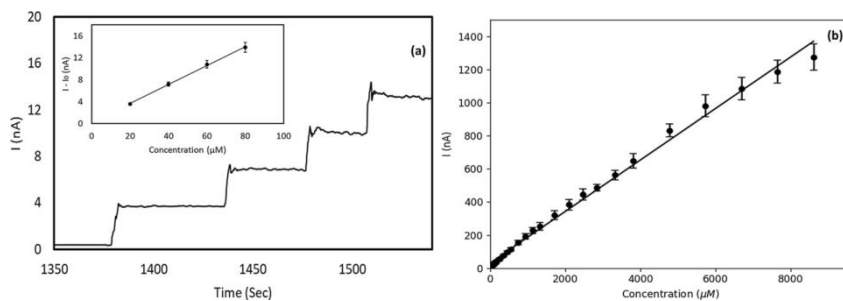


**Figure 5.** (a) Calibration curve created from the amperometric response of a platinum nanoparticle-coated carbon-fiber microelectrode to  $\text{H}_2\text{O}_2$  with a constant potential held at 0.7V vs. Ag/AgCl (3.0 M KCl) over 2000 s; the inset is the calibration curve built of the current response to different concentrations of  $\text{H}_2\text{O}_2$ . (b) Linear range determined in similar fashion by collecting  $\text{H}_2\text{O}_2$  response data from four platinum nanoparticle-coated carbon-fiber microelectrodes. The limit of detection for  $\text{H}_2\text{O}_2$  was determined to be 0.86  $\mu\text{M}$ .<sup>65</sup> Data cropped and reprinted from ref 50 by permission of the publisher.

In amperometry, the potential is held constant at a redox potential for the analyte of interest. Spikes in the current intensity correlate to the detection of the analyte. Due to the frequency of detection being much higher for amperometry than cyclic voltammetry (because

potential scanning is not required), temporal resolution is greatly enhanced.<sup>66</sup> Coupling amperometry with microelectrodes or nanoelectrodes allows for even greater temporal resolution and single-cell spatial resolution. In some cases, these tiny electrodes can penetrate a cell without causing additional stress, allowing for intracellular ROS quantitation.<sup>67</sup>

### ***Electrode coatings***

Major innovations in the electrochemical quantitation of ROS have come primarily from sensor development and electrode coating rather than electrochemical technique innovation. Carbon-fiber microelectrodes (CFMEs) are common sensors for studying single cell events and activity within the brain due to their small size and sensitivity.<sup>68</sup> Although they have historically been used for the detection of common cationic neurotransmitters (dopamine, serotonin, etc), they have proven effective at monitoring reactive oxygen species as well, specifically  $\text{H}_2\text{O}_2$ . The Sombers lab has been using CFMEs to detect  $\text{H}_2\text{O}_2$  since 2010. They first showed a cylindrical CFME to have a 2  $\mu\text{M}$  limit of detection for  $\text{H}_2\text{O}_2$  in a FSCV system with a scan rate of 400 V/s.<sup>69</sup> They advanced on this original paper by coupling  $\text{H}_2\text{O}_2$  and dopamine detection within the tissue of an anesthetized rats' dorsal striatum. By exposing the dorsal striatum to a cell agitation agent (in the case mercaptosuccinic acid), a maximum concentration of 151  $\mu\text{M}$   $\text{H}_2\text{O}_2$  was detected within the tissue. Quantitation was achieved through electrode calibration with known  $\text{H}_2\text{O}_2$  concentrations pumped into the system.<sup>70</sup> To overcome the issue of selective  $\text{H}_2\text{O}_2$  detection, the group electrodeposited 1,3-phenylenediamine onto a bare CFME, creating a size exclusion membrane that prevented other neurochemicals that oxidize at a similar potential to  $\text{H}_2\text{O}_2$  from accessing the electrode, facilitating selective detection down to 5  $\mu\text{M}$   $\text{H}_2\text{O}_2$ .

### ***Metal and nanoparticle coatings***

The working electrode material can be modified to promote enhanced detection of ROS. When considering what material to use, one must think about the potential range of the working electrode, if fouling will be an issue, and how changes in the size of the working electrode will impact detection. Coating the electrode surface is one of the most common methods for enhancing detection capabilities and for improving ROS selectivity and quantitation. Modifications offer the ability to overcome large overpotentials and slow redox kinetics that have historically made electrochemical detection of ROS challenging. Some of the most promising examples of CFME coatings for ROS include platinum, Prussian blue, and metal nanomaterials.  $\text{H}_2\text{O}_2$  reduction is promoted on several of these surfaces, increasing the electrode's sensitivity, and making it one of the most common ROS targets for electrochemical detection. Hu et. al. coated CFMEs in platinum to detect  $\text{H}_2\text{O}_2$  released from isolated single stress granules (membrane-less organelles) using single cell amperometry. The coated electrode was held at an oxidizing potential for  $\text{H}_2\text{O}_2$ , and spike analysis was performed to quantify  $\text{H}_2\text{O}_2$  release kinetics from the stress granules.<sup>71</sup> The study showed enhanced performance from platinum-coated CFMEs compared to a platinum microelectrode or a bare CFME due to the increase in active sites on the coated electrode. In this context, active sites refer to areas of electron transfer between  $\text{H}_2\text{O}_2$  and the working electrode. An increase in active sites means an increase in electrochemical signal and

sensitivity. In this case, platinum nanoparticles have more active sites due to the increased surface area of nanoparticles on the microelectrode.

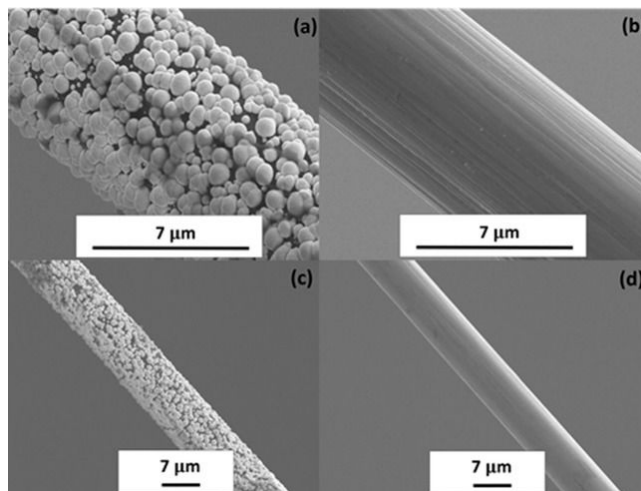


**Figure 6.** Scanning electron microscopy images of platinum nanoparticles coated onto a carbon-fiber microelectrode (a and d) and a bare carbon-fiber microelectrode (b and d) for comparison. Reprinted from ref 50 by permission of the publisher.

Metal nanoparticles have been coated onto CFMEs for  $\text{H}_2\text{O}_2$  detection in several publications. Wang et. al. achieved a limit of detection of  $0.53 \mu\text{M}$   $\text{H}_2\text{O}_2$  by electrodepositing platinum nanoparticles onto the surface of the carbon-fiber (**Figure 6**).<sup>65</sup> Selectivity for  $\text{H}_2\text{O}_2$  was enhanced by further coating the electrodes with polyphenylenediamine and Nafion to create size and charge exclusive layers. Adding these additional coatings increased the limit of detection slightly to  $0.86 \mu\text{M}$   $\text{H}_2\text{O}_2$ , still well within physiological concentrations. Neal et. al. describes a ceria nanoparticle coating on the surface of a silica wafer, achieving an extremely low limit of quantitation for  $\text{H}_2\text{O}_2$  of  $0.1 \text{ pM}$ .<sup>72</sup> The biosensor proved to work over a range of pHs and in solutions with interfering species often found in relevant biological solutions.

### *Enzymatic coatings*

Beyond metal, functionalizing the surface of carbon-fiber and glassy carbon electrodes with enzymes has been a promising innovation for ROS electrochemical detection, especially for intracellular detection. Wang et. al. created a  $\text{C@DNA-Mn}_3(\text{PO}_4)_2$  nanozyme based cell-fixing sensing platform.<sup>73</sup> This mimics an enzyme that can catalyze the reduction of ROS. The specific sensor quantified superoxide down to  $5.87 \text{ nM}$ . In addition to the low limit of detection, cells can be grown on the surface of the electrode to further reduce the response speed from 9 s to 2 s, enhancing the ability to capture short-lived ROS.

Another common electrode coating is cytochrome c (Cyt c). Cyt c is a heme protein found in mitochondria. It is essential for electron transfer and is known to catalyze the reduction of ROS.<sup>74</sup> Thirumalai et. al. improved methods for attaching Cyt c to the glassy carbon electrode surface by creating a colloidal suspension of graphene oxide and Cyt c. Due to the graphene, the colloidal suspension was electrochemically deposited onto the glassy carbon electrode surface,

overcoming a large setback with Cyt c-coated electrodes, sticking it to the surface.<sup>75</sup> Due to the catalytic activity of Cyt c, the electrode was shown to detect  $\text{H}_2\text{O}_2$  down to  $2.3 \mu\text{M}$  and  $\text{O}_2^{\cdot-}$  down to  $6.3 \text{ nM}$ . Enzymatic electrochemical sensors are more likely to react with harder to capture ROS like  $\text{O}_2^{\cdot-}$  and  $\cdot\text{OH}$ , in addition to  $\text{H}_2\text{O}_2$ , because the metal center of several enzymes, especially a heme group, promotes the reduction of ROS, making them advantageous for overcoming the high reactivity of these harder to detect ROS.

### ***Intracellular detection***

One of the most notable advantages to electrochemical quantitation of ROS is the ability to do so intracellularly. The small size and needle-like shape of CFMEs and nanoelectrodes allow penetration through the cell membrane with minimal damage to the cell. Marquitan et. al electrodeposited Prussian Blue onto carbon nanoelectrodes to enhance selectivity for  $\text{H}_2\text{O}_2$  as Prussian Blue lowers the effective reduction potential for  $\text{H}_2\text{O}_2$ .<sup>21</sup> These electrodes were punctured through murine macrophage cell walls, and amperometry was used to detect  $\text{H}_2\text{O}_2$ . They monitored how intracellular  $\text{H}_2\text{O}_2$  concentration levels are impacted by the addition of an extracellular buffer, detecting intracellular  $\text{H}_2\text{O}_2$  concentrations under  $200 \mu\text{M}$ . It is also common to use or functionalize microelectrodes with single walled carbon nanotubes (SWCNTs). Their small size allows for the creation of nano arrays, and the high density of sensor material on the carbon-fiber surface further enhances spatial and temporal resolution. This is a surface area effect, as nanoscale materials always have a surface area advantage over larger materials. Rawson et. al. functionalized an indium tin oxide electrocatalyst with SWCNTs.<sup>76</sup> The SWCNTs attached to an indium tin oxide surface and then functionalized with single strand DNA to enhance the biocompatibility of the sensor. DNA-coated SWCNTs do not cause stress to cells, keeping the production of ROS limited to what is happening naturally. The functionalized SWCNTs were incubated with cells overnight. It was confirmed that the SWCNTs has punctured through the cell membrane while remaining attached to the indium tin oxide surface, allowing the intracellular detection of  $\text{H}_2\text{O}_2$  at extremely fast response times.

### ***Scanning electrochemical microscopy***

A final outstanding electrochemical method for quantifying ROS electrochemically is scanning electrochemical microscopy (SECM). In SECM, a small electrode is scanned across a substrate and collects current responses that are dependent on the electrochemical activity of the substrate and its topography.<sup>77</sup> Its major advantages are the selectivity, spatial resolution, and fast response time, but it suffers from slow overall collection due to the scanning nature of the technique. In order to be successful, SECM require redox mediators. These are redox-active molecules that facilitate SECM measurements. These molecules can be added to an electrolyte solution, although often times molecules already within buffers can suffice. Considering if the redox mediator used will have a biological effect is especially important for cellular ROS measurements, as the addition of a toxic redox mediator could artificially inflate ROS levels within the cells. A common redox mediator for ROS detection within cells is  $\text{Ru}(\text{NH}_3)_6^{3+}$ .<sup>78</sup> Li et. al. describes the direct measurement of several ROS species using SECM with a platinized carbon nanoelectrode tip and  $\text{Ru}(\text{NH}_3)_6^{3+}$  redox mediator.<sup>79</sup> These tips were inserted into the

phagolysosome within cells. By pulsing the potential through four distinct values, the authors were able to extract the individual contributions of four different ROS ( $\text{H}_2\text{O}_2$ ,  $\text{ONOO}^-$ ,  $\text{NO}\cdot$ ,  $\text{NO}_2^-$ ) that were detected within the cells as the tip was scanned through the cell into the phagolysosome. The researchers reported the production rate of each species within phagolysosomes and reported that  $\text{NO}\cdot$  was produced in higher quantities than  $\text{H}_2\text{O}_2$ .

Several SECM ROS detection studies are compromised based on the presence of dissolved oxygen. Dissolved oxygen is necessary for maintaining cellular activity, but it can interfere with ROS detection because several ROS fall beyond dissolved oxygen's reduction potential. To overcome this, Wu et. al. used a platinum ultramicroelectrode with SECM coupled with a multipotential step waveform applied to the tip to determine the concentration of  $\text{H}_2\text{O}_2$  released by cancer cells using a FcMeOH redox mediator.<sup>80, 81</sup> The waveform was designed to detect FcMeOH, dissolved oxygen, and  $\text{H}_2\text{O}_2$  simultaneously. FcMeOH signal was used to locate the tip, while the dissolved oxygen signal was collected so it could be subtracted from the  $\text{H}_2\text{O}_2$  signal, thus eliminating dissolved oxygen interference from the  $\text{H}_2\text{O}_2$  data. The quantitation was achieved by creating a calibration curve with known amounts of  $\text{H}_2\text{O}_2$  and from the SECM data, and it was determined that cancer cells released  $0.85 \mu\text{M}$   $\text{H}_2\text{O}_2$  and normal cells released  $0.28 \mu\text{M}$   $\text{H}_2\text{O}_2$ .

## Electron Paramagnetic Resonance

Electron paramagnetic resonance (EPR), also known as electron spin resonance, is a spectroscopic technique that detects unpaired electrons. Since many reactive oxygen species are free radicals, direct detection of certain ROS is possible with EPR. However, the short lifetime of ROS and low concentrations make direct detection challenging and difficult to realize.<sup>66, 82, 83</sup>

One approach to overcoming these difficulties is incorporating scavengers that react with ROS and form more stable, EPR-active, products. For example, one of the first methods for detecting superoxide and hydroxyl radical was by spin trapping with 5,5-dimethyl-1-pyrroline-N-oxide (DMPO), which forms the stable spin adducts DMPO-OOH and DMPO-OH, respectively.<sup>84</sup> For hydroxyl radical, the formation of the DMPO-OH complex increased the lifetime of the radical species from  $10^{-9}$  s to 30 min, making detection with EPR possible.<sup>85</sup> It should be noted that if a large portion of the generated ROS are scavenged, systems may be perturbed by the resulting changes in ROS levels leading to skewed experimental results.

Quantifying ROS in a system is determined by changes in the EPR spectrum following reactions with ROS. The most common EPR probes, such as nitrones and cyclic hydroxylamines, operate in a turn-on fashion where the scavengers are EPR-silent until reacting with ROS and becoming EPR-active, leading to an increase in signal proportional to ROS concentration.<sup>86, 87</sup> The intensity of the EPR signal is related to the number of spins present, providing an avenue for quantitation (**Figure 7**). Typically, a radical calibration curve is created from a stable radical species such as 4-hydroxy-TEMPO (TEMPOL) to establish a relationship between signal intensity and spin concentration. In certain circumstances, internal standards with known spin concentrations (such as  $\text{Mn}^{2+}$ ) can be incorporated to further standardize spin intensities.<sup>87, 88</sup> Frequently, quantitation is reported in concentration of the oxidized EPR-active species, which can correspond to a certain ROS concentration depending on selectivity and the EPR probe used. However, quantitation is also reported in concentration of "oxidants," total ROS, or number of

spins as opposed to a molarity. Since ROS probes only capture a fraction of all ROS generated, it is important the percentage captured remains constant over time to accurately compare across conditions.

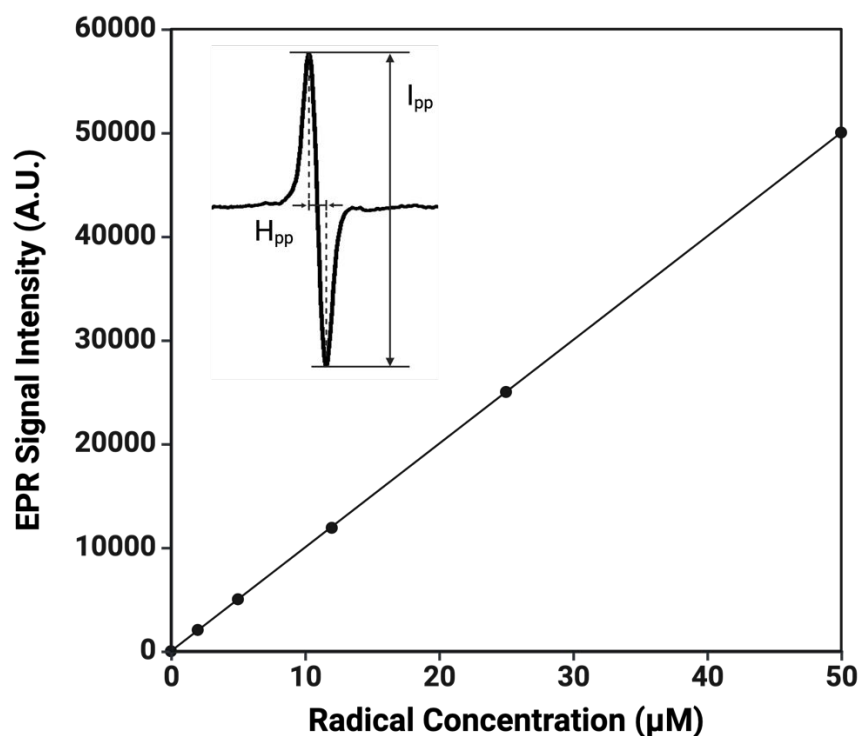


**Figure 7.** Calibration curve example generated from known radical concentrations and the resulting EPR signal intensity. Inset EPR signal highlights different methods for defining signal intensity.  $I_{pp}$  is peak-to-peak signal height,  $H_{pp}$  is the peak-to-peak- linewidth. Double integration of signals is also used, which integrates the signal once to get the absorption spectrum and again to obtain the area under the curve. This is required since EPR signals are presented as a first derivative spectrum.

EPR is widely accepted and used in both biological and non-biological systems as a method for quantifying ROS. Sample types amenable to EPR range from simple solutions to biological tissues and organisms. Spatial information and resolution are limited with EPR, samples are prepared in tubes and inserted into an EPR cavity without any imaging components. Any spatial information about ROS localization in cells is a result of using spin traps or probes that target specific cellular regions. Most EPR spectrometers have sensitivity in the low  $\mu\text{M}$  range ( $10^{-7}$  -  $10^{-8}$  M); limits of detection and the timeframe of each measurement is heavily dependent on acquisition parameters.<sup>82, 89</sup> Progress in quantifying ROS using EPR is less explicitly about improving LODs/LOQs, and more about establishing a system with reliable quantitation for specific ROS. Research towards improving quantitation of ROS has generally focused on (1) optimizing spin traps or spin probes and (2) sample preparation, instrumentation, and methodology. Additionally, throughout the past 10 years, a great deal of effort has gone towards fundamentally understanding interactions between spin traps/probes and ROS, elucidating reaction mechanisms, and identifying potential side reactions or interference. The major questions

researchers are answering today surround quantifying ROS accurately and confidently. Thus, this portion of the review will highlight critical progress in understanding how to use EPR for quantifying ROS and important methodology considerations.

### Spin traps and spin probes

Generally, there are two types of scavengers used in EPR for ROS detection: spin traps and spin probes. Spin traps, which are typically nitrones like DMPO, form a covalent bond with the ROS free radical through a radical addition reaction to form a spin adduct (**Figure 8**). Covalent bond formation results in spin adduct products dependent on ROS identity with distinct EPR spectra. However, with DMPO, differentiation between superoxide and hydroxyl radical is challenging since the superoxide adduct (DMPO-OOH) readily decomposes to the hydroxyl radical adduct (DMPO-OH) and other species.<sup>90, 91</sup>

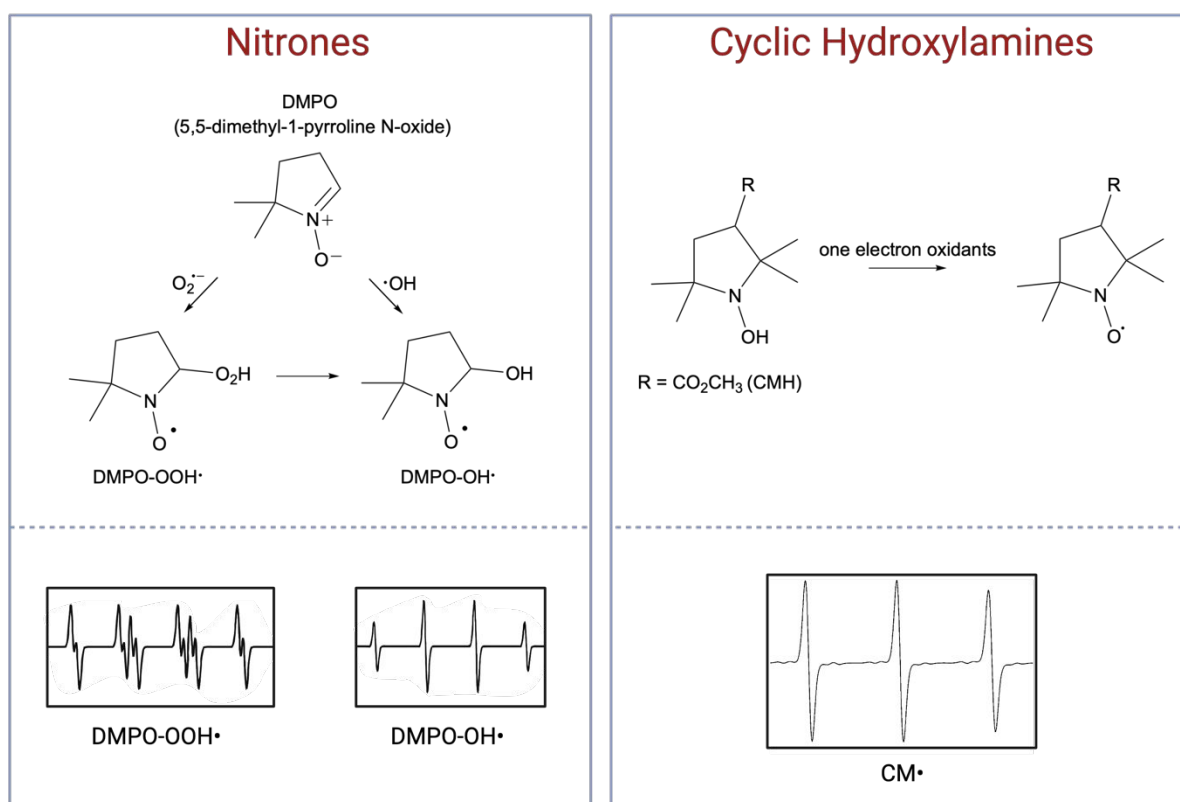


**Figure 8.** Example reactions between nitrones (spin traps) and cyclic hydroxylamine (spin probes) with ROS and the resulting EPR spectra. For nitrones, reactions with superoxide and hydroxyl radical form separate products due to covalent bond formation. This results in different EPR spectra; however, the superoxide adduct actively transforms to the hydroxyl adduct. Cyclic hydroxylamines undergo a one electron oxidation regardless of ROS, forming the same EPR spectrum. DMPO-OOH and DMPO-OH spectra cropped from ref 74.<sup>92</sup> and licensed under CC BY 4.0. CM $\cdot$  spectra cropped from ref 75. and licensed under CC BY 4.0.<sup>93</sup>



Spin traps react with superoxide at relatively slow rates, making accurate quantitation challenging due to competition with cellular antioxidants like superoxide dismutase (SOD) and ascorbate that may react with superoxide faster than the spin trap can.<sup>3</sup> The slow rate constants also require using high concentrations of spin traps (20 - 100 mM), which can perturb cellular systems and affect cell viability.<sup>91</sup> Additionally, intracellular reductants such as ascorbate and ferric hemeproteins can reduce the spin adducts to EPR-silent products under certain conditions and lead to artificially lower signals.<sup>90, 91</sup>

Spin probes on the other hand are typically cyclic hydroxylamines that undergo one-electron oxidation to produce a nitroxide radical, which is the product regardless of ROS identity. The reactions between superoxide and cyclic hydroxylamines form nitroxides, which show increased stability compared to spin adducts, and proceed at rates roughly two orders of magnitude faster than spin traps ( $10^3$ - $10^4$  M<sup>-1</sup>s<sup>-1</sup> vs. 30 and 70 M<sup>-1</sup>s<sup>-1</sup>).<sup>3</sup> Strong EPR signals can be obtained with much lower cyclic hydroxylamine concentrations (25-500 μM) than with spin probes, resulting in lower toxicity and cellular disruptions.<sup>86</sup> As a result, the high reactivity of cyclic hydroxylamines and resulting nitroxide stability allows for intracellular superoxide detection.<sup>86</sup>

For both spin traps and probes, measurements are typically attributed to certain types of ROS only after validation with specific inhibitors or scavengers. For example, with DMPO, superoxide dismutase (SOD) is used to determine what portion of the signal is from superoxide vs. hydroxyl radical. This is particularly critical for spin probes as any one-electron oxidant can oxidize the probe.<sup>90</sup>

Each spin trap and spin probe operates optimally under different conditions and can provide different insight into a system. Various studies have explicitly compared spin traps and probes in similar systems to identify which performs best. Sheinok et. al. compared the sensitivity and specificity for detecting superoxide (vs. hydroxyl radical) in buffer, cell lysates, and cells across many EPR probes (TEMPOL, mitoTEMPO, trityl CT-03, CMH, mitoTEMPO-H, and DIPPMPO) (**Figure 9**).<sup>94</sup> CT-03 was highly specific for superoxide, but was not very sensitive (only detecting ~50% superoxide in buffer and <10% in cell lysates). DIPPMPO and CMH were the best candidates for selectively and sensitively detecting superoxide in complex biological media. Additionally, both DIPPMPO and CMH present membrane permeability allowing them to detect both intracellular and extracellular superoxide.

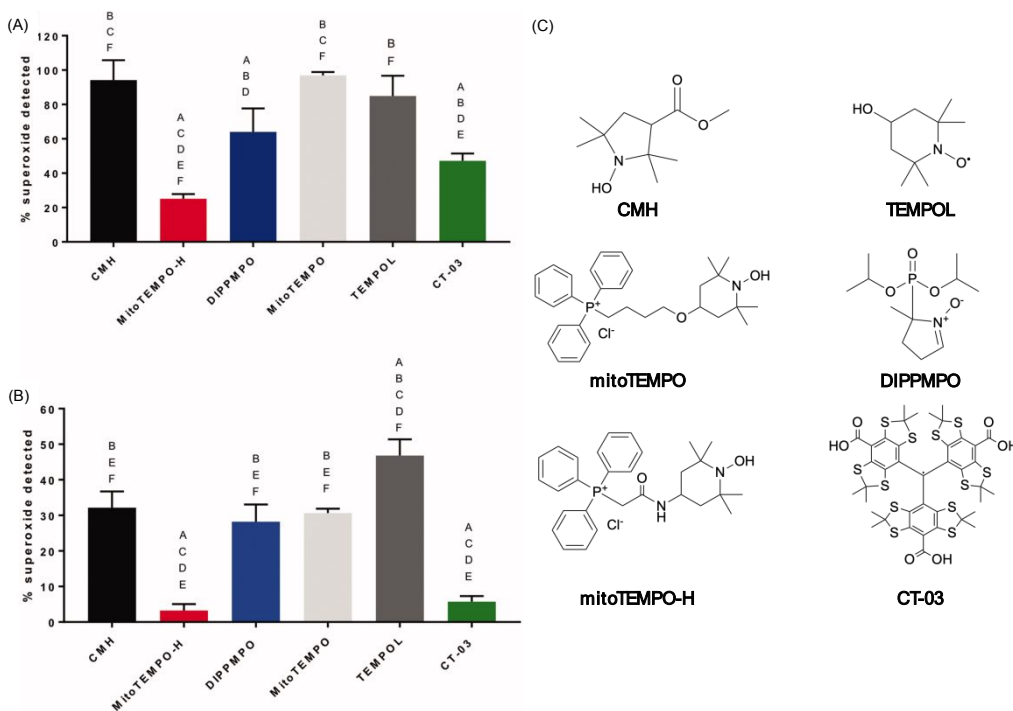


**Figure 9.** Percentage of superoxide detected by different probes after 10 min compared to generated superoxide in (A) PBS media and (B) in cell lysates. Reprinted from ref 77 by permission of the publisher. (C) Shows the chemical structure of the various probes used.

### Spin traps

General trends in spin trap development have focused on ROS specificity and selectivity, increasing spin adduct stability, and modifications for cellular localization. For example, electron-withdrawing groups at position 5 (in molecules such as DEPMPO, DIPPMPPO, BMPO, or EMPO) have been shown to improve the stability of spin adducts in buffer. Similarly, the superoxide adducts of DEPMPO derivatives with a triphenylphosphonium group (Mito-DEPMPO and Mito-DIPPMPPO) or permethylated B-cyclodextrin (CD-DEPMPO and CD-DIPPMPPO) have also shown increased stability and persistence.<sup>95</sup> Various moieties can also improve cellular localization, such as triphenylphosphonium groups which allow mitochondrial accumulation.<sup>96</sup>

Abbas et. al. compared new (Mito-DIPPMPPO and CD-DIPPMPPO) and commonly used (DMPO, BMPO, DEPMPO, and DIPPMPPO) cyclic nitron spin traps to detect superoxide in stimulated and unstimulated RAW macrophages (RAW 264.7 cells).<sup>95</sup> In buffer with a constant flux of superoxide radical ( $2.8 \pm 0.3 \mu\text{M}/\text{min}$ ), DMPO detected a steady-state concentration of superoxide ( $1 \mu\text{M}$ ) whereas BMPO, DEPMPO, DIPPMPPO, and Mito-DIPPMPPO detected at a rate of  $0.8\text{--}1.2 \pm 0.2 \mu\text{M}/\text{min}$ . The CD-DIPPMPPO adduct performed the best, with a rate of  $1.5 \pm 0.2 \mu\text{M}/\text{min}$ , and successfully detected superoxide in stimulated and unstimulated cells ( $80 \pm 10 \text{ pmol}/10^6 \text{ cells}/\text{min}$  vs.  $3 \pm 2 \text{ pmol}/10^6 \text{ cells}/\text{min}$ ). Additional studies indicated CD-DIPPMPPO was not internalized by the cells, suggesting all superoxide production was extracellular, contrary to past studies with hydroxylamines that suggest negligible superoxide release by RAW macrophages.<sup>97</sup>

Interactions with media can influence ROS and spin adduct stability and should be taken into consideration when monitoring ROS in a system. More complex matrices contain components

that can interfere with spin probes and ROS, resulting in reduced ROS concentrations being detected. For example, Chauvin et. al. analyzed ROS generated by He plasma in water, and DMEM with and without fetal calf serum (FCS).<sup>98</sup> Hydroxyl radical concentrations were detected through the spin adduct DMPO-OH at 4.12  $\mu\text{M}$ , 3  $\mu\text{M}$ , and 0.4  $\mu\text{M}$  in water, DMEM, and DMEM+FCS, respectively. The amount of ROS detected was dependent on the media, where the highest amount of DMPO-OH observed was in water. They hypothesize that in cell culture media, hydroxyl radical can react with organic components such as amino acids, vitamins, and proteins, lowering the quantities of  $\cdot\text{OH}$  trapped by DMPO. Additionally, the DMPO-OH adduct stability was 2 times lower in the presence of FCS than in water or DMEM, indicating other potential avenues for decreased detection.

Outside of biological systems, challenges still arise when using spin traps to quantify ROS.<sup>88, 99-102</sup> In electrochemical advanced oxidation processes (EAOP), DMPO can be electrochemically oxidized into DMPO-OH (the same spin adduct that would form if hydroxyl radical was present).<sup>103</sup> Pei et. al. worked to establish DMPO concentrations necessary to effectively spin trap  $\cdot\text{OH}$  and obtain reliable EPR signals in EAOP.<sup>88</sup> High concentrations of DMPO (>125 mM) improved the trapping efficiency of  $\cdot\text{OH}$  by kinetically inhibiting other paramagnetic species forming and preferentially forming DMPO-OH. They also studied the impact of trapping time, since the DMPO-OH adduct, while longer living than  $\cdot\text{OH}$ , is still susceptible to natural decay. Trapping times longer than 300 s resulted in decreased DMPO-OH signals and increased signals of interferential species – highlighting the importance of trapping time in accurate quantification. Jeong et. al. studied the stability of spin adducts from hydroxyl radical (DMPO-OH), superoxide anion (BMPO-OOH), and singlet oxygen (TPC- $^1\text{O}_2$ ) and published recommendations emphasizing the importance in considering spin adduct lifetime and incubation time.<sup>100</sup>

Other potential avenues for interference in quantification include metal oxides and Fenton chemistry.<sup>99, 101</sup> Metal oxides can react with DMPO and form DMPO-OH even when ROS are not present.<sup>99</sup> In Fenton chemistry, when using DMPO to monitor  $\cdot\text{OH}$  production, DMPO-OH can be further oxidized by  $\text{Fe}^{3+}$ , reducing the DMPO-OH signal.<sup>101</sup> As a result, concentrations of DMPO should be 20 times higher than  $[\text{H}_2\text{O}_2]$  and 200 times higher than iron to get a reliable EPR signal for monitoring  $\cdot\text{OH}$  production.

### *Spin probes*

Similar to spin traps, spin probes are often modified for cellular localization, such as with triphenylphosphonium moieties for mitochondrial targeting.<sup>96, 104</sup> Sheinok et. al. modified CMH, one of the most frequently used and efficient spin probes, with triphenylphosphonium to form mitoCPH, and compared superoxide sensitivity with CMH and mito-TEMPO-H. In PBS buffer, mitoCPH and CMH captured almost all generated superoxide, however, in cell lysates CMH performed the best but still captured less than 40% of the generated superoxide.<sup>96</sup> This highlights how challenging it is to accurately quantify ROS in complex matrices. Even with what may be considered proper controls, there may be apparent differences in ROS concentrations not resulting from any true difference in ROS production.

### **Methodology**

The experimental protocols and conditions, such as temperature, buffers, oxygen content, metal chelators, and more, play a large role in ROS quantification reliability and EPR probe

sensitivity. Since there is not a universal standard method for ROS detection, many research groups use slightly different parameters making comparisons across studies very challenging. In 2020, Gotham et. al. investigated the effect of different conditions on the autoxidation of CMH and DMPO to establish optimal conditions for cell studies.<sup>90</sup> They found that the additional metal ions present in buffers greatly increased the rate of spin probe autoxidation, suggesting buffers be simplified as long as they are fulfilling experimental needs. Additionally, metal chelators can be added to reduce autoxidation and improve sensitivity, as long as the chelators are biocompatible with the system of interest. At optimized conditions, CMH still showed significant autoxidation whereas DMPO exhibited minimal autoxidation. As a result, the CMH method was not sensitive enough to detect ROS generation in stimulated RAW264.7 cells, while DMPO was, challenging previous conclusions that CMH and spin probes are more sensitive than DMPO and spin traps. Moving forward, EPR probe autoxidation must be considered and, where relevant, subtracted from ROS generation rates for accurate quantification.

Freezing samples is frequently used to increase flexibility between when experiments are conducted and EPR measurements are performed.<sup>105</sup> When using frozen samples, low temperature EPR measurements are employed to reduce potential freeze-thaw changes that may accompany room temperature measurements. Gotham et. al. found that the stable radical standards showed good linear regression between frozen and room temperature samples, despite much lower signal intensities.<sup>90</sup> However, along with lower signal intensities, CMH also showed inconsistencies between frozen and room temperature samples, raising questions on the accuracy and sensitivity of low temperature storage and measurement. In addition, freezing tissues disrupts membranes and alters ion concentrations such that ROS production is not necessarily proportional to the level that was initially generated.<sup>66</sup> For accurate quantification, EPR measurements should be carried out at consistent time intervals as soon as possible and under relevant conditions.

Along with experimental protocols and conditions, proper spectrometer acquisition parameters are critical for obtaining the good signal-to-noise required for accurate quantification. Makino et. al. reported variabilities in signal with different sample tubes and holders, sample volumes, solvents, and position in the cavity.<sup>87</sup> If all of these parameters were consistent over every run, EPR intensity was reproduced with an error of 2% or less for  $\mu\text{M}$  samples. They also noted that for low concentrations, a flat quartz cuvette may yield better signal intensity. Thus, all experimental stages are critical for ensuring accurate quantification of ROS.

## Conclusions and field recommendations

Major enhancements in the field of ROS quantitation have primarily been in the development of new fluorescence and EPR probes and electrode coatings. Although these enhancements have overcome several limitations in the field, further development will be necessary to confidently and specifically quantitate ROS in the wide variety of contexts where ROS are known to be important.

Within fluorescence detection, enhancing the specificity and potential for quantitation with ROS fluorescent probes has been a major development over the last ten years. Other luminescent probes such as chemiluminescent and phosphorescent probes have also been developed with similar speed and spatial resolution advantages to their fluorescent counterparts.<sup>73, 106</sup> Even with these advances, there are several interfering species that can quench or enhance luminescent

signal; this makes absolute quantitation impossible as multiple species are contributing to the signal. Fluorescence is still most useful for detecting signal changes rather than accurately quantifying a molecule.<sup>107-109</sup> More complex probes need to be developed to deter the effects of a complex sample. Examples of these probes include several fluorescent chemosensors, which show promising selectivity and sensitivity to a variety of ROS. This is especially true regarding trace ROS detection in tissue and cell samples.

Another way to improve ROS detection is to couple fluorescence with a technique that is better-suited for absolute quantitation, such as electrochemistry or EPR. The real novelty of fluorescent detection is its fast detection times, simple sample preparation, and spatial determination of analytes in biological samples (when imaging). If the imaging power and low detection limits of fluorescence were coupled with a technique with high specificity and accurate quantitation, it would make a powerful analysis method for ROS. However, combining two analytical methods to yield complementary information in registry is challenging. For example, one must consider sample conservation to limit sample perturbation for both methods. Often, more quantitative techniques require more excessive and intrusive sample preparation. Conducting two methods sequentially for ROS detection is challenging as the sample changes at such short timescales, making *in vivo* or *in situ* quantitation unreliable. Thus, tandem *in vivo* or *in situ* analysis methods are the future for ROS detection.

Electrochemical techniques provide direct, quantitative, and real-time detection of ROS, though limited by the redox potentials of specific ROS with particular electrode configurations. Over the last ten years, electrode coatings have provided a method to overcome specificity problems. Coating basic electrode materials provides enhanced sensitivity and selectivity for ROS. Enzymatic coatings overcome pH detection restrictions because different enzymes can function in different pH windows and allow for detection within a wide range of biological samples without interference due to enzyme specificity. Even with several types of coatings, the majority of literature focuses on detecting ROS other than  $\cdot\text{OH}$ , which remains too short-lived to detect reliably with electrochemical techniques. In the future, electrochemical detection of a trapped species may allow hydroxyl radical detection. Challenges remain in specificity, dual detection, and consistency across a range of environmental variables. Electrochemical techniques are extremely sensitive to changes in temperature, pH, electrolyte and background species, as well as electrode material; this creates challenges in detection across studies if all variables are not reported.

The predominant methods for quantifying ROS using EPR is through spin traps and spin probes which readily react with ROS to form stable products that are then measured with EPR. In the past decade, research has focused on both developing new probes and increasing fundamental understandings of how probes work to ensure accurate ROS quantitation and detection. The predominate variables that influence ROS quantitation include potential probe transformations, interference from other species and the system at large, incubation time with probes, sample preparation, and instrument parameters. However, with a detailed understanding of the necessary parameters and restrictions for the specific probe being used, proper controls, and consistent protocols, EPR is a highly powerful tool for ROS quantitation. Additional work should be done across the field to establish consistent protocols so that measured ROS concentrations can be compared more broadly. Spatial resolution remains challenging with EPR as any spatial information is typically obtained through probes with cellular targets or isolating cellular components. Aside from developing new probes with cellular targeting, instrumentation needs to improve for additional spatial and temporal resolution.

In general, these major detection techniques continue to suffer from poor selectivity. Probe development continues to fill this gap, but often leads to more complex detection systems that can act as a barrier to access for non-specialists and can limit detection in more complex environmental and biological solutions. Likewise, the reactivity and short lifetimes of ROS remain a challenge for the consistency of detection, especially in biological systems. For example, H<sub>2</sub>O<sub>2</sub> can be produced as a byproduct of superoxide generation in mitochondria and H<sub>2</sub>O<sub>2</sub> can break down into ·OH, making it difficult to know the true source of ROS from a biological or environmental sample. Therefore, it is important for researchers to take these limitations into consideration, especially when the goal is a mechanistic understanding of possible sources of ROS. Likewise, many of these detection methods may underestimate the amount of ROS produced due to interfering species, and there is still concern about ensuring that the detection method is not an additional source of ROS to the system. However, if researchers keep in mind these limitations, acknowledge them appropriately, and couple them with ongoing developments in quantitation methods, ROS can be quantitated confidently. This quantitation is key towards driving the understanding of several biological, medicinal, and industrial processes forward.

### Author Contributions

Eleni Spanolios – Conceptualization, writing- original draft (introduction, fluorescence, electrochemical, and conclusion), writing – review and editing, visualization, supervision  
Riley Lewis – Writing – original draft (fluorescence, EPR), writing – review and editing,  
Rhea Caldwell – Writing – original draft (fluorescence)  
Safia Z. Jilani – Writing – original draft (fluorescence)  
Christy Haynes – Writing- review and editing, funding acquisition

### Data Availability

No primary research results, software or code have been included and no new data were generated or analysed as part of this review

### Conflicts of Interest

The authors declare they have no competing financial or personal interests to disclose.

### Acknowledgements

This work was supported by the National Science Foundation under grant no. CHE2001611, the NSF Center for Sustainable Nanotechnology (CSN). The CSN is part of the Centers for Chemical Innovation Program. SZJ would like to acknowledge support from the Ford Foundation Postdoctoral Fellowship to contribute to this work. REL is supported the ACS Division of Analytical Chemistry and Agilent. Figure 1 and the TOC were created using biorender.com.

### Notes and References

1. K. Krumova and G. Cosa, *Compr Ser Photoch*, 2016, **13**, 3-21.
2. X. Chen, F. Wang, J. Y. Hyun, T. Wei, J. Qiang, X. Ren, I. Shin and J. Yoon, *Chem Soc Rev*, 2016, **45**, 2976-3016.
3. S. I. Dikalov and D. G. Harrison, *Antioxid Redox Signal*, 2014, **20**, 372-382.
4. Y. Nosaka and A. Y. Nosaka, *Chem Rev*, 2017, **117**, 11302-11336.

5. G. Yu, Y. Wang, H. Cao, H. Zhao and Y. Xie, *Environ Sci Technol*, 2020, **54**, 5931-5946.
6. S. Mansoor, O. Ali Wani, J. K. Lone, S. Manhas, N. Kour, P. Alam, A. Ahmad and P. Ahmad, *Antioxidants (Basel)*, 2022, **11**.
7. R. Mittler, S. I. Zandalinas, Y. Fichman and F. Van Breusegem, *Nat Rev Mol Cell Biol*, 2022, **23**, 663-679.
8. C. Waszczak, M. Carmody and J. Kangasjarvi, *Annu Rev Plant Biol*, 2018, **69**, 209-236.
9. B. Kalyanaraman, V. Darley-Usmar, K. J. Davies, P. A. Dennery, H. J. Forman, M. B. Grisham, G. E. Mann, K. Moore, L. J. Roberts, 2nd and H. Ischiropoulos, *Free Radic Biol Med*, 2012, **52**, 1-6.
10. Y. Zhang, M. Dai and Z. Yuan, *Analytical Methods*, 2018, **10**, 4625-4638.
11. C. P. Rubio and J. J. Ceron, *BMC Vet Res*, 2021, **17**, 226.
12. J. Li, M. Jiang, H. Zhou, P. Jin, K. M. C. Cheung, P. K. Chu and K. W. K. Yeung, *Glob Chall*, 2019, **3**, 1800058.
13. M. D. Bartberger, W. Liu, E. Ford, K. M. Miranda, C. Switzer, J. M. Fukuto, P. J. Farmer, D. A. Wink and K. N. Houk, *Proc Natl Acad Sci U S A*, 2002, **99**, 10958-10963.
14. R. Radi, *J Biol Chem*, 2013, **288**, 26464-26472.
15. K. Das and A. Roychoudhury, *Frontiers in Environmental Science*, 2014, **2**.
16. S. H. Audi, N. Friedly, R. K. Dash, A. M. Beyer, A. V. Clough and E. R. Jacobs, *Free Radic Res*, 2018, **52**, 1052-1062.
17. N. Wang, C. J. Miller, P. Wang and T. D. Waite, *Anal Chim Acta*, 2017, **963**, 61-67.
18. V. Shcherbakov, S. A. Denisov and M. Mostafavi, *RSC Adv*, 2023, **13**, 8557-8563.
19. A. A. Abubaker, D. Vara, I. Eggleston, I. Canobbio and G. Pula, *Platelets*, 2019, **30**, 181-189.
20. H. Gunawardena, R. Silva and P. Ranasinghe, *BMC Res Notes*, 2019, **12**, 809.
21. M. Marquitan, J. Clausmeyer, P. Actis, A. L. Córdoba, Y. Korchev, M. D. Mark, S. Herlitze and W. Schuhmann, *ChemElectroChem*, 2016, **3**, 2125-2129.
22. S. Mondal, R. B. Jethwa, B. Pant, R. Hauschild and S. A. Freunberger, *Faraday Discuss*, 2024, **248**, 175-189.
23. A. Gomes, E. Fernandes and J. L. Lima, *J Biochem Biophys Methods*, 2005, **65**, 45-80.
24. F. Rezende, R. P. Brandes and K. Schroder, *Antioxid Redox Signal*, 2018, **29**, 585-602.
25. S. Dikalov, K. K. Griendling and D. G. Harrison, *Hypertension*, 2007, **49**, 717-727.
26. H. J. Forman, O. Augusto, R. Brigelius-Flohe, P. A. Dennery, B. Kalyanaraman, H. Ischiropoulos, G. E. Mann, R. Radi, L. J. Roberts, 2nd, J. Vina and K. J. Davies, *Free Radic Biol Med*, 2015, **78**, 233-235.
27. A. J. Kowaltowski, *Redox Biol*, 2019, **21**, 101065.
28. D. Sharan, D. Wolfson, C. M. Green, P. Lemke, A. G. Gavin, R. J. Hamers, Z. V. Feng and E. E. Carlson, *Environmental Science: Nano*, 2023, **10**, 1978-1992.
29. M. Madhu, S. Santhoshkumar, W.-B. Tseng and W.-L. Tseng, *Frontiers in Analytical Science*, 2023, **3**.
30. L. Wu, L. Liu, H.-H. Han, X. Tian, M. L. Odyniec, L. Feng, A. C. Sedgwick, X.-P. He, S. D. Bull and T. D. James, *New Journal of Chemistry*, 2019, **43**, 2875-2877.
31. Garima, S. Jindal, S. Garg, I. Matai, G. Packirisamy and A. Sachdev, *Mikrochim Acta*, 2021, **188**, 13.
32. M. Zhang, T. Wang, X. Lin, M. Fan, Y. Zho, N. Li and X. Cui, *Sensors and Actuators B: Chemical*, 2021, **331**.
33. X. Jia, Q. Chen, Y. Yang, Y. Tang, R. Wang, Y. Xu, W. Zhu and X. Qian, *J Am Chem Soc*, 2016, **138**, 10778-10781.
34. P. Wang, L. Yu, J. Gong, J. Xiong, S. Zi, H. Xie, F. Zhang, Z. Mao, Z. Liu and J. S. Kim, *Angew Chem Int Ed Engl*, 2022, **61**, e202206894.
35. H. Liu, W. Chen, W. Yuan, J. Gao, Q. Zhang, P. Zhang and C. Ding, *Sensors and Actuators B: Chemical*, 2023, **379**.

36. G. Yang, Z. Liu, R. Zhang, X. Tian, J. Chen, G. Han, B. Liu, X. Han, Y. Fu, Z. Hu and Z. Zhang, *Angew Chem Int Ed Engl*, 2020, **59**, 16154-16160.
37. Y. Tang, Y. Su, N. Yang, L. Zhang and Y. Lv, *Anal Chem*, 2014, **86**, 4528-4535.
38. H. Chen, D. Li, Y. Zheng, K. Wang, H. Zhang, Z. Feng, B. Huang, H. Wen, J. Wu, W. Xue and S. Huang, *Spectrochim Acta A Mol Biomol Spectrosc*, 2024, **309**, 123733.
39. W. Yao, Y. Cao, M. She, Y. Yan, J. Li, X. Leng, P. Liu, S. Zhang and J. Li, *ACS Sens*, 2021, **6**, 54-62.
40. W. Feng, Y. Zhang, Z. Li, S. Zhai, W. Lv and Z. Liu, *Anal Chem*, 2019, **91**, 15757-15762.
41. J. Yang, X. Liu, H. Wang, H. Tan, X. Xie, X. Zhang, C. Liu, X. Qu and J. Hua, *Analyst*, 2018, **143**, 1242-1249.
42. N. Kwon, Y. Hu and J. Yoon, *ACS Omega*, 2018, **3**, 13731-13751.
43. D. Wu, A. C. Sedgwick, T. Gunnlaugsson, E. U. Akkaya, J. Yoon and T. D. James, *Chem Soc Rev*, 2017, **46**, 7105-7123.
44. L. Wu, A. C. Sedgwick, X. Sun, S. D. Bull, X. P. He and T. D. James, *Acc Chem Res*, 2019, **52**, 2582-2597.
45. Q. Xu, C. H. Heo, G. Kim, H. W. Lee, H. M. Kim and J. Yoon, *Angew Chem Int Ed Engl*, 2015, **54**, 4890-4894.
46. X. Sun, Q. Xu, G. Kim, S. E. Flower, J. P. Lowe, J. Yoon, J. S. Fossey, X. Qian, S. D. Bull and T. D. James, *Chemical Science*, 2014, **5**.
47. R. R. Nazarewicz, A. Bikineyeva and S. I. Dikalov, *J Biomol Screen*, 2013, **18**, 498-503.
48. Q. Han, J. Liu, Q. Meng, Y.-L. Wang, H. Feng, Z. Zhang, Z. P. Xu and R. Zhang, *ACS Sensors*, 2018, **4**, 309-316.
49. A. S. M. Islam, M. Sasmal, D. Maiti, A. Dutta, B. Show and M. Ali, *ACS Omega*, 2018, **3**, 10306-10316.
50. K. Kundu, S. F. Knight, N. Willett, S. Lee, W. R. Taylor and N. Murthy, *Angew Chem Int Ed Engl*, 2009, **48**, 299-303.
51. Z. Zhu, H. Ding, Y. Wang, C. Fan, Y. Tu, G. Liu and S. Pu, *Tetrahedron*, 2020, **76**.
52. M. Mondal, R. Das, R. Pal, S. Nag and P. Banerjee, *Journal of Materials Chemistry A*, 2024, **12**, 21626-21676.
53. L. Wang, H. Lin, B. Yang, X. Jiang, J. Chen, S. Roy Chowdhury, N. Cheng, P. A. Nakata, D. M. Lonard, M. C. Wang and J. Wang, *J Am Chem Soc*, 2024, **146**, 22396-22404.
54. Z. Yu, Q. Li, J. Wang, Y. Yu, Y. Wang, Q. Zhou and P. Li, *Nanoscale Res Lett*, 2020, **15**, 115.
55. O. Adegoke and P. B. Forbes, *Anal Chim Acta*, 2015, **862**, 1-13.
56. R. Ma, G. Lin, Y. Zhou, Q. Liu, T. Zhang, G. Shan, M. Yang and J. Wang, *npj Computational Materials*, 2019, **5**.
57. R. J. Wydra, P. G. Rychahou, B. M. Evers, K. W. Anderson, T. D. Dziubla and J. Z. Hilt, *Acta Biomater*, 2015, **25**, 284-290.
58. V. A. Sadhu, S. Jha, T. J. Park and S. K. Kailasa, *J Fluoresc*, 2024, DOI: 10.1007/s10895-023-03578-5.
59. S. Zhao, G. Zang, Y. Zhang, H. Liu, N. Wang, S. Cai, C. Durkan, G. Xie and G. Wang, *Biosens Bioelectron*, 2021, **179**, 113052.
60. A. V. Geraskevich, A. N. Solomonenko, E. V. Dorozhko, E. I. Korotkova and J. Barek, *Crit Rev Anal Chem*, 2024, **54**, 742-774.
61. S. Borgmann, *Anal Bioanal Chem*, 2009, **394**, 95-105.
62. N. Elgrishi, K. J. Rountree, B. D. McCarthy, E. S. Rountree, T. T. Eisenhart and J. L. Dempsey, *Journal of Chemical Education*, 2017, **95**, 197-206.
63. C. Batchelor-McAuley, E. Katelhon, E. O. Barnes, R. G. Compton, E. Laborda and A. Molina, *ChemistryOpen*, 2015, **4**, 224-260.
64. P. Puthongkham and B. J. Venton, *Analyst*, 2020, **145**, 1087-1102.



65. B. Wang, X. Wen, P. Y. Chiou and N. T. Maidment, *Electroanalysis*, 2019, **31**, 1641-1645.
66. M. P. Murphy, H. Bayir, V. Belousov, C. J. Chang, K. J. A. Davies, M. J. Davies, T. P. Dick, T. Finkel, H. J. Forman, Y. Janssen-Heininger, D. Gems, V. E. Kagan, B. Kalyanaraman, N. G. Larsson, G. L. Milne, T. Nystrom, H. E. Poulsen, R. Radi, H. Van Remmen, P. T. Schumacker, P. J. Thornalley, S. Toyokuni, C. C. Winterbourn, H. Yin and B. Halliwell, *Nat Metab*, 2022, **4**, 651-662.
67. C. Amatore, S. Arbault, C. Bouton, K. Coffi, J. C. Drapier, H. Ghandour and Y. Tong, *Chembiochem*, 2006, **7**, 653-661.
68. M. Hejazi, W. Tong, M. R. Ibbotson, S. Praver and D. J. Garrett, *Front Neurosci*, 2021, **15**, 658703.
69. S. W. M. Audrey L. Sanford, Kelsey L. Whitehouse, Hannah M. Oara, Leyda Z. Lugo-Morales, James G. Roberts, and Leslie A. Sombers, *Analytical Chemistry*, 2010, **82**, 5205-5210.
70. M. Spanos, J. Gras-Najjar, J. M. Letchworth, A. L. Sanford, J. V. Toups and L. A. Sombers, *ACS Chem Neurosci*, 2013, **4**, 782-789.
71. K. Hu, E. Relton, N. Locker, N. T. N. Phan and A. G. Ewing, *Angew Chem Int Ed Engl*, 2021, **60**, 15302-15306.
72. C. J. Neal, A. Gupta, S. Barkam, S. Saraf, S. Das, H. J. Cho and S. Seal, *Sci Rep*, 2017, **7**, 1324.
73. Y. Wang, D. Wang, L. H. Sun, L. C. Zhang, Z. S. Lu, P. Xue, F. Wang, Q. Y. Xia and S. J. Bao, *Anal Chem*, 2020, **92**, 15927-15935.
74. M. Huttemann, P. Pecina, M. Rainbolt, T. H. Sanderson, V. E. Kagan, L. Samavati, J. W. Doan and I. Lee, *Mitochondrion*, 2011, **11**, 369-381.
75. D. Thirumalai, V. Kathiresan, J. Lee, S. H. Jin and S. C. Chang, *Analyst*, 2017, **142**, 4544-4552.
76. F. J. Rawson, J. Hicks, N. Dodd, W. Abate, D. J. Garrett, N. Yip, G. Fejer, A. J. Downard, K. H. Baronian, S. K. Jackson and P. M. Mendes, *ACS Appl Mater Interfaces*, 2015, **7**, 23527-23537.
77. D. Polcari, P. Dauphin-Ducharme and J. Mauzeroll, *Chem Rev*, 2016, **116**, 13234-13278.
78. S. E. Salamifar and R. Y. Lai, *Anal Chem*, 2013, **85**, 9417-9421.
79. Y. Li, K. Hu, Y. Yu, S. A. Rotenberg, C. Amatore and M. V. Mirkin, *J Am Chem Soc*, 2017, **139**, 13055-13062.
80. T. Wu, X. Ning, Q. Xiong, F. Zhang and P. He, *Electrochimica Acta*, 2022, **403**.
81. X. Ning, T. Wu, Q. Xiong, F. Zhang and P. G. He, *Anal Chem*, 2020, **92**, 12111-12115.
82. F. A. F. Menezes, J. G. Oliveira and A. O. Guimarães, *Applied Magnetic Resonance*, 2023, **55**, 335-355.
83. H. F. V. Victoria, D. C. Ferreira, J. B. G. Filho, D. C. S. Martins, M. V. B. Pinheiro, G. A. M. Safar and K. Krambrock, *Free Radic Biol Med*, 2022, **180**, 143-152.
84. E. Finkelstein, G. M. Rosen and E. J. Rauckman, *Arch Biochem Biophys*, 1980, **200**, 1-16.
85. S. H. Chae, M. S. Kim, J. H. Kim and J. D. Fortner, *ACS ES T Eng*, 2023, **3**, 1504-1510.
86. S. I. Dikalov, Y. F. Polienko and I. Kirilyuk, *Antioxid Redox Signal*, 2018, **28**, 1433-1443.
87. Y. Makino, M. Ueno, Y. Shoji, M. Nyui, I. Nakanishi, K. Fukui and K. I. Matsumoto, *J Clin Biochem Nutr*, 2022, **70**, 213-221.
88. S. Pei, S. You, J. Ma, X. Chen and N. Ren, *Environ Sci Technol*, 2020, **54**, 13333-13343.
89. S. Malacrida, F. De Lazzari, S. Mrakic-Sposta, A. Vezzoli, M. A. Zordan, M. Bisaglia, G. M. Menti, N. Meda, G. Frighetto, G. Bosco, T. Dal Cappello, G. Strapazzon, C. Reggiani, M. Gussoni and A. Megighian, *Biol Open*, 2022, **11**.

90. J. P. Gotham, R. Li, T. E. Tipple, J. R. Lancaster, Jr., T. Liu and Q. Li, *Free Radic Biol Med*, 2020, **154**, 84-94.
91. K. Abbas, N. Babic and F. Peyrot, *Methods*, 2016, **109**, 31-43.
92. L. Vojta, D. Caric, V. Cesar, J. Antunovic Dunic, H. Lepedus, M. Kveder and H. Fulgosi, *Sci Rep*, 2015, **5**, 10085.
93. J. Czwartos, B. Dobosz, W. Kasprzycka, P. N. Osuchowska, M. Stepinska, E. A. Trafny, J. Starzynski and Z. Mierczyk, *Int J Mol Sci*, 2023, **24**.
94. S. Scheinok, P. Leveque, P. Sonveaux, B. Driesschaert and B. Gallez, *Free Radic Res*, 2018, **52**, 1182-1196.
95. K. Abbas, M. Hardy, F. Poulhes, H. Karoui, P. Tordo, O. Ouari and F. Peyrot, *Free Radic Biol Med*, 2014, **71**, 281-290.
96. S. Scheinok, B. Driesschaert, D. d'Hose, P. Sonveaux, R. Robiette and B. Gallez, *Free Radic Res*, 2019, **53**, 1135-1143.
97. A. M. Palazzolo-Ballance, C. Suquet and J. K. Hurst, *Biochemistry*, 2007, **46**, 7536-7548.
98. J. Chauvin, F. Judee, M. Yousfi, P. Vicendo and N. Merbahi, *Sci Rep*, 2017, **7**, 4562.
99. J.-H. Wu and H.-Q. Yu, *Environmental Science & Technology Letters*, 2024, **11**, 370-375.
100. M. S. Jeong, K. N. Yu, H. H. Chung, S. J. Park, A. Y. Lee, M. R. Song, M. H. Cho and J. S. Kim, *Sci Rep*, 2016, **6**, 26347.
101. J. M. Fontmorin, R. C. Burgos Castillo, W. Z. Tang and M. Sillanpaa, *Water Res*, 2016, **99**, 24-32.
102. Y. Zong, L. Chen, Y. Zeng, J. Xu, H. Zhang, X. Zhang, W. Liu and D. Wu, *Environ Sci Technol*, 2023, **57**, 9394-9404.
103. E. Braxton, D. J. Fox, B. G. Breeze, J. J. Tully, K. J. Levey, M. E. Newton and J. V. Macpherson, *ACS Meas Sci Au*, 2023, **3**, 21-31.
104. J. Zielonka, J. Joseph, A. Sikora, M. Hardy, O. Ouari, J. Vasquez-Vivar, G. Cheng, M. Lopez and B. Kalyanaraman, *Chem Rev*, 2017, **117**, 10043-10120.
105. K. Berg, M. Ericsson, M. Lindgren and H. Gustafsson, *PLoS One*, 2014, **9**, e90964.
106. J. S. Kim, K. Jeong, J. M. Murphy, Y. A. R. Rodriguez and S. S. Lim, *Oxid Med Cell Longev*, 2019, **2019**, 1754593.
107. Z. Xu, S. Liu, L. Xu, Z. Li, X. Zhang, H. Kang, Y. Liu, J. Yu, J. Jing, G. Niu and X. Zhang, *Anal Chim Acta*, 2024, **1297**, 342303.
108. X. Zhou, Y. Kwon, G. Kim, J. H. Ryu and J. Yoon, *Biosens Bioelectron*, 2015, **64**, 285-291.
109. J. Chang, Y. Wang, X. Kong, B. Dong and T. Yue, *Anal Chim Acta*, 2024, **1298**, 342410.

No primary research results, software or code have been included and no new data were generated or analysed as part of this review.